OPEN ACCESS

Fluoroscopy-guided high-intensity focused ultrasound ablation of the lumbar medial branch nerves: dose escalation study and comparison with radiofrequency ablation in a porcine model

Michael Gofeld ,[1] Thomas Tiennot,[2] Eric Miller,[3] Niv Rebhun,[3] Stephen Mobley,[3] Suzanne Leblang,[4] Ron Aginsky,[5] Arik Hananel,[3] Jean-Francois Aubry[6]

► Additional supplemental material is published online only. To view, please visit the journal online (https://doi.org/10.1136/rapm-2024-105417).

[1]Unika Medical Centre, Toronto, Ontario, Canada
[2]INSERM Physics for Medicine Paris, Paris, France
[3]FUS Mobile, Alpharetta, Georgia, USA
[4]Focused Ultrasound Foundation, Charlottesville, Virginia, USA
[5]FUSMobile LTD, Haifa, Israel
[6]Physics for Medicine Paris, INSERM, Paris, France

Correspondence to
Dr Michael Gofeld, Unika Medical Centre , Toronto, Canada; mikegofeld@gmail.com

Received 23 February 2024
Accepted 11 March 2024

To cite: Gofeld M, Tiennot T, Miller E, *et al*. *Reg Anesth Pain Med* Epub ahead of print: [*please include* Day Month Year]. doi:10.1136/rapm-2024-105417

ABSTRACT

Background Radiofrequency ablation (RFA) is a common method for alleviating chronic back pain by targeting and ablating of facet joint sensory nerves. High-intensity focused ultrasound (HIFU) is an emerging, non-invasive, image-guided technology capable of providing thermal tissue ablation. While HIFU shows promise as a potentially superior option for ablating sensory nerves, its efficacy needs validation and comparison with existing methods.

Methods Nine adult pigs underwent fluoroscopy-guided HIFU ablation of eight lumbar medial branch nerves, with varying acoustic energy levels: 1000 (N=3), 1500 (N=3), or 2000 (N=3) joules (J). An additional three animals underwent standard RFA (two 90 s long lesions at 80°C) of the same eight nerves. Following 2 days of neurobehavioral observation, all 12 animals were sacrificed. The targeted tissue was excised and subjected to macropathology and micropathology, with a primary focus on the medial branch nerves.

Results The percentage of ablated nerves with HIFU was 71%, 86%, and 96% for 1000 J, 1500 J, and 2000 J, respectively. In contrast, RFA achieved a 50% ablation rate. No significant adverse events occurred during the procedure or follow-up period.

Conclusions These findings suggest that HIFU may be more effective than RFA in inducing thermal necrosis of the nerve.

WHAT IS ALREADY KNOWN ON THIS TOPIC

⇒ High-intensity focused ultrasound (HIFU) can be used in lieu of the radiofrequency ablation (RFA) method to ablate tissue. However, a direct in vivo comparison between these two methods has never been attempted.

WHAT THIS STUDY ADDS

⇒ This animal study evaluated the macroanatomy and microanatomy of HIFU and RFA lesions and confirmed that HIFU produced a more reliable medial branch neurotomy in a porcine model.

HOW THIS STUDY MIGHT AFFECT RESEARCH, PRACTICE OR POLICY

⇒ The results suggest that further HIFU clinical research is anatomically justified, and the method may eventually replace RFA in interventional pain practice.

INTRODUCTION

Back pain is the second-leading symptom prompting all physician visits in the USA.[1] The etiology is often multifactorial and may be linked to musculoskeletal, neurological, and behavioral causes, fitting the biopsychosocial concept of chronic pain. However, discrete pain generators, such as the lumbar facet joints, can be addressed by therapeutic interventions based on a proper selection of candidates. The cited prevalence of lumbar facet joint pain ranges from as low as 4.8% in the multicenter national low back pain survey to over 50% in systemic reviews.[2] A conservative clinically sound estimation of the prevalence of painful degenerative spondyloarthropathy (figure 1A) is hovering at about 15%.[3 4]

Radiofrequency ablation (RFA) of the medial branch nerves of the dorsal primary rami is an effective minimally invasive therapeutic option providing long-lasting pain relief and functional improvement.[2] However, RFA may be associated with an aggravation of pain, injury to the spinal cord or nerve roots, and bleeding.[2 4] Although, the infection rate was not specifically addressed in the published surveys, theoretically, any invasive procedure has a risk of contamination. Special considerations for patients with implanted electrical devices and adjacent metallic hardware are required.[2 5] In addition, the withholding heparin and heparinoids before invasive spine procedures such as RFA has been strongly recommended,[6] and a shared decision model was recommended for other anticoagulants and antiaggregants.[2]

High-intensity focused ultrasound (HIFU) is a novel, non-invasive, image-guided thermal ablation technology[7 8] that has been introduced as an alternative to achieve the same goal as RFA.[9–11] Using an extracorporeal transducer, ultrasound energy is focused on a target location, much like a magnifying glass converges light to a single point to ignite a fire. The concentration of energy generates coagulative necrosis precisely in the targeted volume while sparing near-field and far-field tissue.[12]

Therefore, HIFU can be used as another method for thermal neurotomy[13–15] and potentially be more

advantageous than RFA. However, a direct in vivo comparison between these two methods has never been attempted.

The goal of this study was to compare an escalating dose of HIFU versus RFA as a tool for neurotomy of the lumbar medial branch nerves using simulation, clinical follow-up, and histopathology.

METHODS

Acoustic and thermal simulations

The thermal rise induced by the focused ultrasound beam at the neural target was modelled with a simulation following the method previously described by Chen *et al*[16]; therefore, it is described here in brief and additional detail can be found in online supplemental materials. The propagation of the ultrasound beam through the tissues was simulated, and the root mean square pressure field was used as the input heat source for the thermal simulation. The acoustic power of the simulation was scaled based on calibrated measurements in water (see online supplemental materials).

Simulations were carried out at 15° to the sagittal plane to better match the experimental treatment geometry.[17] A graphics processing unit (Nvidia Quadro RTX 8000) was used with k-Wave's accelerated solver. Specific details about the k-Wave pseudospectral implementation of the wave equations can be found in the literature.[18]

To assess the thermal effect on tissue, we used the concept of thermal dose,[19] which is the thermal analog of the radiation dose used in radiotherapy.[20] Thermal dose is given in units of cumulative equivalent minutes at 43°C (CEM43).

A lesion threshold map was generated contouring where the voxels exceed 240 CEM43, which is a conservative threshold for thermal ablation.[21] The dimensions of the resulting lesion were measured and compared with histological observations.

Three energy levels were simulated: 1000 J, 1500 J, and 2000 J, corresponding to 50 s duration at 20, 30, and 40 watts (W), respectively. For each energy level, eight lesions were generated using bilateral targets on the four lumbar vertebrae.

Procedures

12 healthy female swine (Sus scrofa domestica) 3–4 months old of mixed breed (LargeWhite X LandRace) and weighing 42±5 kg were acquired from LAHAV C.R.O. (The Institute of Animal Research), in Israel.

Nine pigs underwent medial branch nerve ablation with HIFU at four vertebral levels bilaterally while the other three pigs underwent RFA at the same levels (table 1).

A total of 72 fluoroscopy-guided HIFU ablations were performed in nine pigs with 1000 J (N=3), 1500 J (N=3), and 2000 J (N=3). A total of 24 ablations in three pigs were performed with RFA.

HIFU and RFA procedures were performed using C-arm fluoroscopy for guidance (12-inch Arcadis Aventic, Siemens Healthineers, Erlangen, Germany).

HIFU ablation was performed using the Neurolyzer XR prototype (Neurolyzer XR, FUSMobile, Alpharetta, Georgia, USA), a 1-MHz HIFU device[16] consisting of the following components: control unit, positioner, HIFU transducer, and imaging workstation. The workstation provided graphical targeting overlay. The control unit was located beside the user during treatment and connected to the HIFU transducer.

Before each procedure, the pigs were fasted for 24 hours, underwent baseline neurological evaluation, and were weighed. Animals were anesthetized in a pain-free and stress-free manner and placed in a prone position. The pig's hair was removed from the skin overlaying L1–L6 with shaving and depilatory cream (Veet cream), and the area was rinsed with soap and water. Vital signs and pain-related cardiovascular responses were continuously monitored with procedure pause and pain mitigation used where needed.

The known anatomic location of the nerve at the junction of the transverse process and the superior articular process (SAP) was targeted by tilting the C-Arm 10°–15°.

Ultrasonic gel (Aquasonic 100 ultrasound gel, Parker Laboratories, USA) mixed with water was applied to the skin along with a proprietary coupling gel pad (FUSMobile, Alpharetta, Georgia, USA, figure 1B). A positioner containing the therapeutic transducer (figure 1C) and aiming accessory (figure 1D) was placed on top of the gel pad. Using the predicted targeting overlay generated by the imaging workstation, the acoustic beam was aligned with the anatomic target.

After alignment was confirmed by repeating the fluoroscopy image (figure 1E), a lateral view at 90° relative to the positioner verified the targeting depth (figure 1F, red lines).

At each of the four target locations, a single ablation sonication was performed with a total energy of either 1000 J, 1500 J, or 2000 J. At the end of each procedure, the animal's back was evaluated for skin changes prior to transfer to their enclosure for observation.

RFA was performed using acceptable clinical methodology and a commercially available device (Neurotherm NT2000iX, Abbott, Austin, Texas, USA). The image intensifier was positioned in anterior–posterior (AP) view, and the vertebral endplates were rectified. The position was adjusted for each vertebral level. An 18-gauge radiofrequency cannula with 10 mm curved active tip was inserted laterally and inferiorly to the target and advanced until bone contact was made. The cannula was aimed at the base of the SAP. After the cannula contacted the bone surface, the image intensifier was rotated to a lateral view and the cannula was further advanced along the inferior part of the SAP (figure 1G). Before beginning RFA, another AP image was acquired to confirm the final cannula placement (figure 1H). The stylet was removed, and the probe was introduced into the cannula. Motor stimulation at 2 Hz was performed up to 1.5 mV. No lower extremity muscle stimulation was seen. Multifidi muscle contractions were strong and visible at 0.2–0.3 mV. A standard RFA protocol of two lesions (90 s at 80°C), with active tip 90° rotation between lesions, was performed.

After the study interventions, the animals woke up and were extubated. After confirming stable vital signs, the animals were transferred to their enclosures.

During the follow-up visits, the pigs were monitored for general behavior, intake of food and water, and neurological deficits. At the end of the 2-day follow-up period, the animals were sacrificed using potassium chloride injection under intravenous anesthesia.

Postprocedure analyses

The tissue specimens (lumbar vertebrae L1–L6 and surrounding soft tissues) were excised en bloc and placed in formalin 10%. During tissue harvest, the intervertebral disks were localized under fluoroscopy, and deep transverse cuts were made in the soft tissues denoting the borders of each vertebra.

Following fixation, each segment was cut into approximately 5 mm thick slices (including the spinal cord, vertebrae, and surrounding soft tissue) using a diamond wheel saw and were evaluated for gross pathology. The gross pathology evaluation

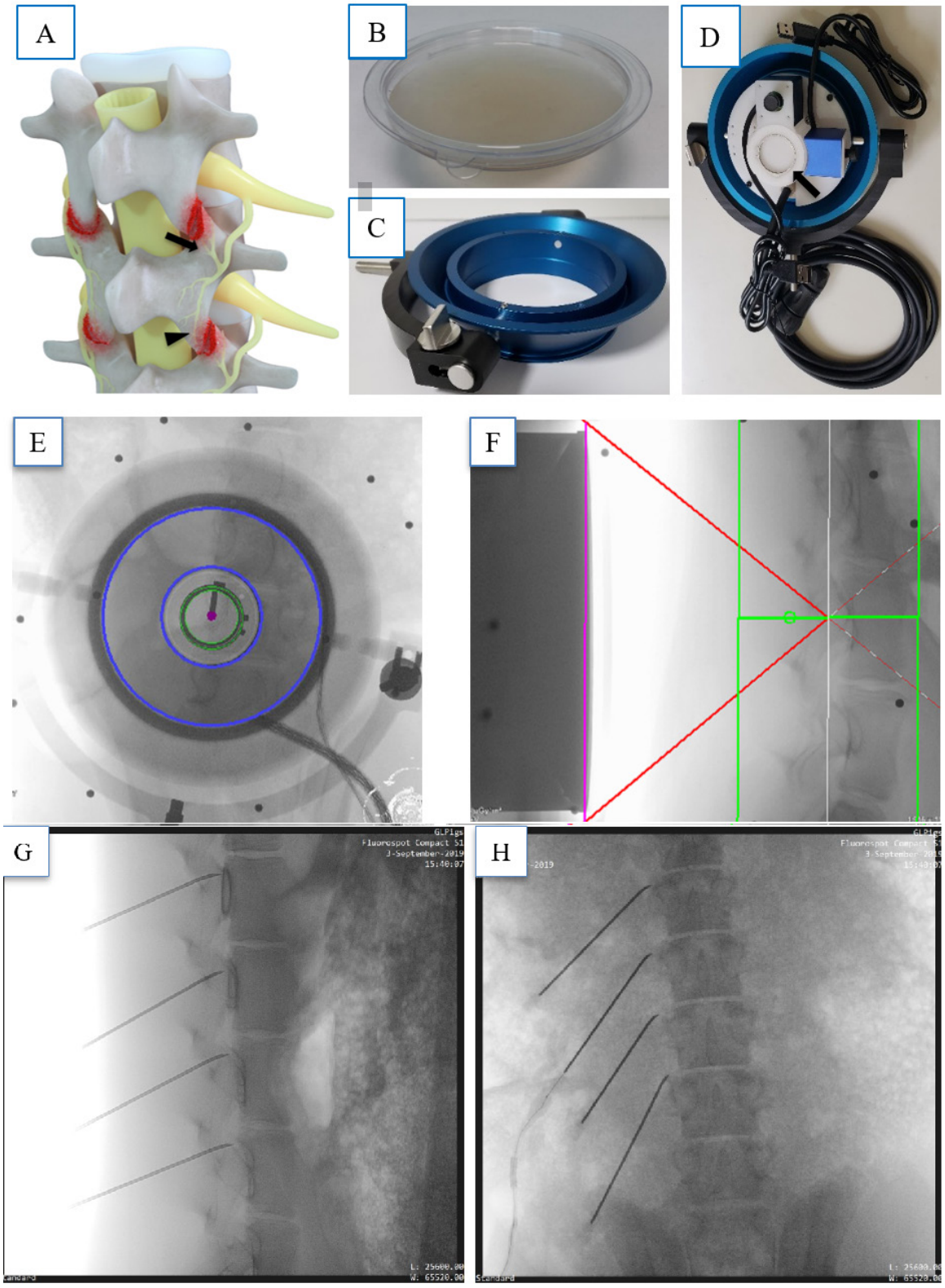

Figure 1 (A) Lumbar spondylosis: the model demonstrates facet degeneration in red. The proximal medial branch nerve supplies sensory innervation to the ipsilateral facet joint just inferior to the neural foramen (black arrow) while the distal medial branch nerve innervates the facet joint more inferiorly (black arrowhead). (B) Disposable coupling gel pad. (C) Cradle. (D) Neurolyzer positioner, which includes the therapeutic transducer inside the cradle along with the aiming system; central rings for target localization (black arrow) and adjacent top (white) and side (blue) camera boxes for assisting with right-to-left and superior-inferior aiming. (E) AP fluoroscopic image confirms HIFU targeting. The pink dot overlays the target location of the medial branch nerve along the lateral aspect of the pedicle inside the two concentric green rings. (F) Lateral fluoroscopic image confirms that the red lines from the margins of the HIFU transducer converge at the simulated target location. The green lines delineate the depth of the treatment envelope. (G) Fluoroscopic imaging of lateral view and (H) AP views confirmed cannulae positions prior to RFA. AP, anterior–posterior; HIFU, high-intensity focused ultrasound; RFA, radiofrequency ablation.

Table 1 Medial branch nerve ablations, locations and parameters per treatment group

Pig ID	Treatment type/energy		Ablated nerves
8997	HIFU 1000 J	Left L2–L5, right L2–L5	7/8
8998	HIFU 1000 J	Left L2–L5, right L2–L5	6/8
9024	HIFU 1000 J	Left L1–L4, right L2–L5	4/8
Total:			17/24=71%
8996	HIFU 1500 J	Left L2–L5, right L2–L5	8/8
9000	HIFU 1500 J	Left L2–L5, right L2–L5	6/8
9002*	HIFU 1500 J	Left L1–L4, right L1–L4	5/6
Total:			19/22=86%
8994	HIFU 2000 J	Left L2–L5, right L2–L5	8/8
9001	HIFU 2000 J	Left L2–L5, right L2–L5	8/8
9025	HIFU 2000 J	Left L2–L5, right L2–L5	7/8
Total:			23/24=96%
8993	RFA	Left L2–L5, right L2–L5	6/8
8995	RFA	Left L2–L5, right L2–L5	3/8
8999	RFA	Left L2–L5, right L2–L5	3/8
Total:			12/24=50%

*In pig 9002, treatment was performed bilaterally at the L1–L4 levels instead of L2–L5 due to variable pig anatomy (pigs typically have six but may have only five lumbar vertebra). As we excised and evaluated L2–L5, on pathology we were only able to document 5/8 lesions in this pig (70/72 total).
HIFU, high-intensity focused ultrasound; RFA, radiofrequency ablation.

was performed by a veterinarian scientist and one of the authors (RA). Thermal lesion size and location were measured, and inclusion of the targeted medial branch nerve was documented. Slices with thermal lesions were placed in super-mega cassettes for decalcification and processing.

Histopathological processing and analysis included H&E staining and immunohistochemistry staining using an antibody (Ab) against myelin basic protein (MBP). In this study, MBP antibody was used for staining the spinal cord and the medial branch nerves to observe thermal effects.

Although each lesion extended through several slides, we selected the slide with the maximal lesion size before performing H&E histology on the selected slide. Depending on the targeted anatomy and energy level used, the HIFU lesion shape appeared as either a pyramid with its flat base positioned on the bone surface, or a crescent-like lesion with the curvature nestled in the junction of the transverse process and the base of the facet process.

The estimation of thermal damage to the targeted medial branch nerves and surrounding tissue took into account the effects of heat fixation.[22–24]

RESULTS

Postprocedure observation

All 12 pigs behaved normally with no visible limping and developed no neurological deficits. They exhibited full energy and appetite throughout the follow-up period. Skin appeared intact with no evidence of damage.

Pathology

On average, the HIFU procedure induced medial branch nerve ablation in 84% of the cases. The effect was dose-dependent, reaching 71%, 86%, and 96% with 1000 J, 1500 J, and 2000 J, respectively. RFA produced thermal damage of the target nerve in 50% of the cases. These results are shown in table 1.

Figure 2 shows the macropathology of thermal lesions at the target location (figure 2A,B), along with images from the H&E (figure 2C,E) and MBP slides (2D,F) following HIFU and RFA ablation. Notably, the MBP staining included the medial branch nerves within an area of necrosis after the HIFU procedure (heat fixed, figure 2D) and along the periphery of the necrotic area after RFA (figure 2F). An additional evaluation was performed on Pig 9001 (2000 J) to evaluate the existence and extent of heat fixation. An experienced in the phenomenon pathologist examined the slices under a polarized light microscope and confirmed the nerve cells were indeed necrotic.

Some post-RFA slices demonstrated hemorrhage in the belly of multifidus muscles, possibly due to mechanical trauma (figure 3A). Another example (figure 3B,C) shows the RFA lesion in soft tissues with medial branch nerves outside the area of ablation. Post-HIFU macropathology and micropathology displayed a broad-based lesion along the bone surface with the medial branch nerve within the area of necrosis (figure 3D,E).

Analysis of lesion size

Figure 4 shows the increase in lesion width as HIFU energy increases, which closely follows the simulation prediction. An average lesion width of 11.0 mm (±2.6 mm, n=22), 12.6 mm (±2.7 mm, n=21), and 12.9 mm (±3.6 mm, n=20) was measured at energies of 1000 J, 1500 J, and 2000 J, respectively. The average lesion width for RFA was 8.0 mm (±1.5 mm, n=22). With HIFU, there was no damage to tissue outside the target location.

Acoustic simulation

We simulated the lesion width and height for each of the three power levels. The results of these simulations (figure 4) show the same trend as the HIFU procedure: higher energy creates a larger lesion. In addition, simulation of a HIFU lesion using a target depth (77 mm), energy (1000 J), and acoustic power (20 W) demonstrated an 18% larger lesion along a confluence of bony surfaces as compared with a flat, bony surface.

Also, per simulation, temperature rise was rapid at the bone–soft tissue interface, crossing the 80°C threshold a few seconds after sonication started at all power levels.

DISCUSSION

This animal study evaluated the safety, and macropathology and micropathology of medial branch nerve ablation with HIFU at escalating energies and compared the results with RFA. No significant adverse events occurred in either the HIFU or RFA groups.

A dose-dependent increase in the rate of medial branch nerve ablation was observed with increasing HIFU energies, from the typical clinical levels used in current clinical trials (1000 J) up to the system maximum output (2000 J). All three HIFU energy levels demonstrated more reliable medial branch nerve ablation and larger lesions than RFA. Larger lesions have a higher probability of including the nerves and ablating a more extended segment of the nerve, which may, in turn, result in more reliable and longer-lasting pain relief.[13 25–27]

The anatomic target for RFA is the base of the SAP,[27] and the cannula is placed adjacent to the bone surface and the target nerve. However, the medial branch nerve resides within 100–200 µm of the bone and may have some variable trajectory. RFA is dependent on tissue electrical impedance, electric current distribution, electrode orientation, and other factors.[28] With RFA, maximum ablation occurs near the active tip of the cannula

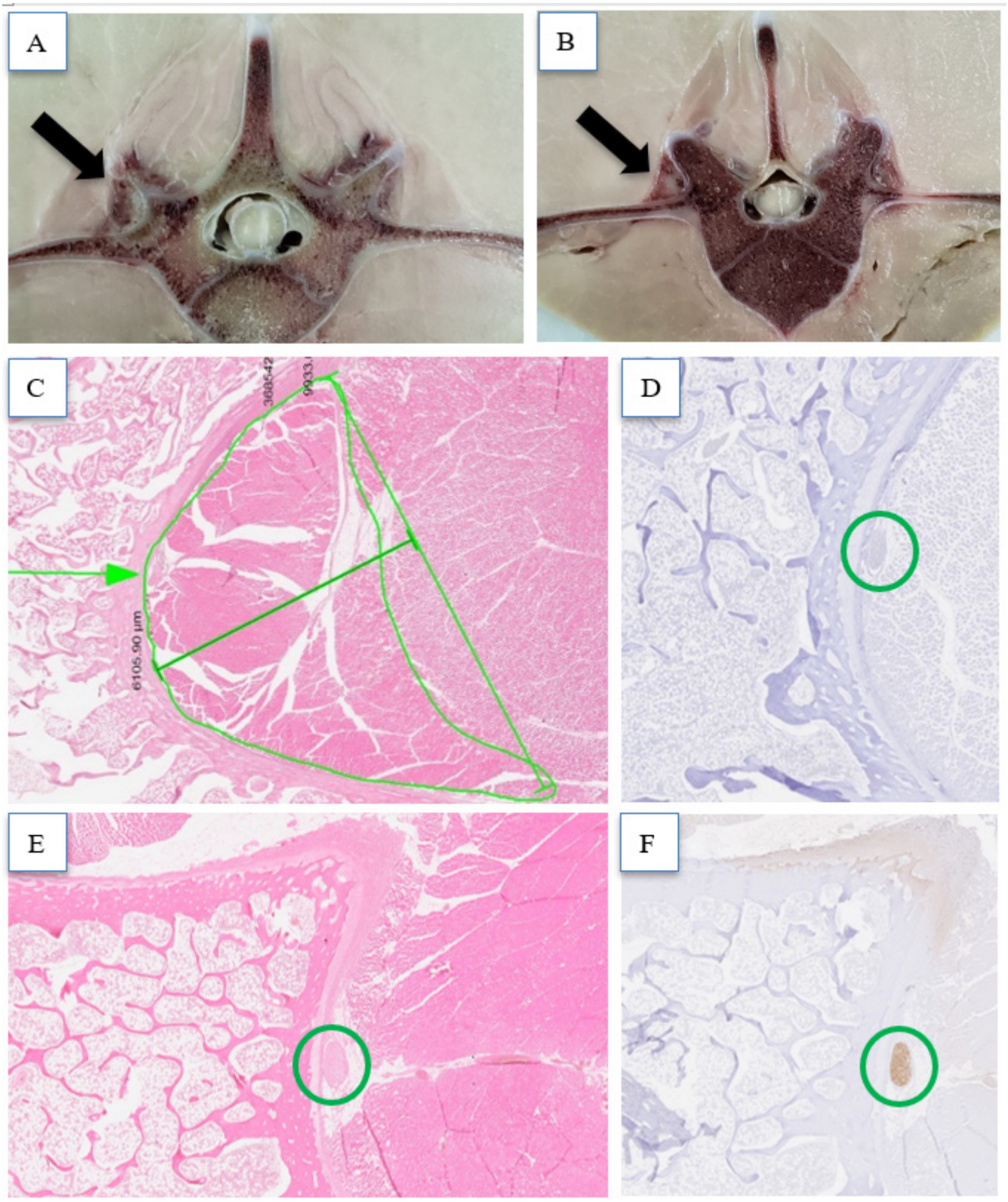

Figure 2 Macropathology demonstrates lesion formation at the proximal medial branch nerve location following (A) HIFU and (B) RFA (black arrows). Histology demonstrates the HIFU lesion on H&E stain (C) creates a large area of necrosis along the bony surface (outlined in green) with the proximal medial branch nerve located along the bony surface within the area of necrosis (green arrow) confirmed using MBP stain (small green circle, (D). The RFA lesion on H&E stain (E) reveals necrosis in the soft tissues near the bone with the proximal medial branch nerve (green circle) located outside and medial to the area of necrosis confirmed using MBP stain (small green circle, (F). HIFU, high-intensity focused ultrasound; MBP, myelin basic protein; RFA, radiofrequency ablation.

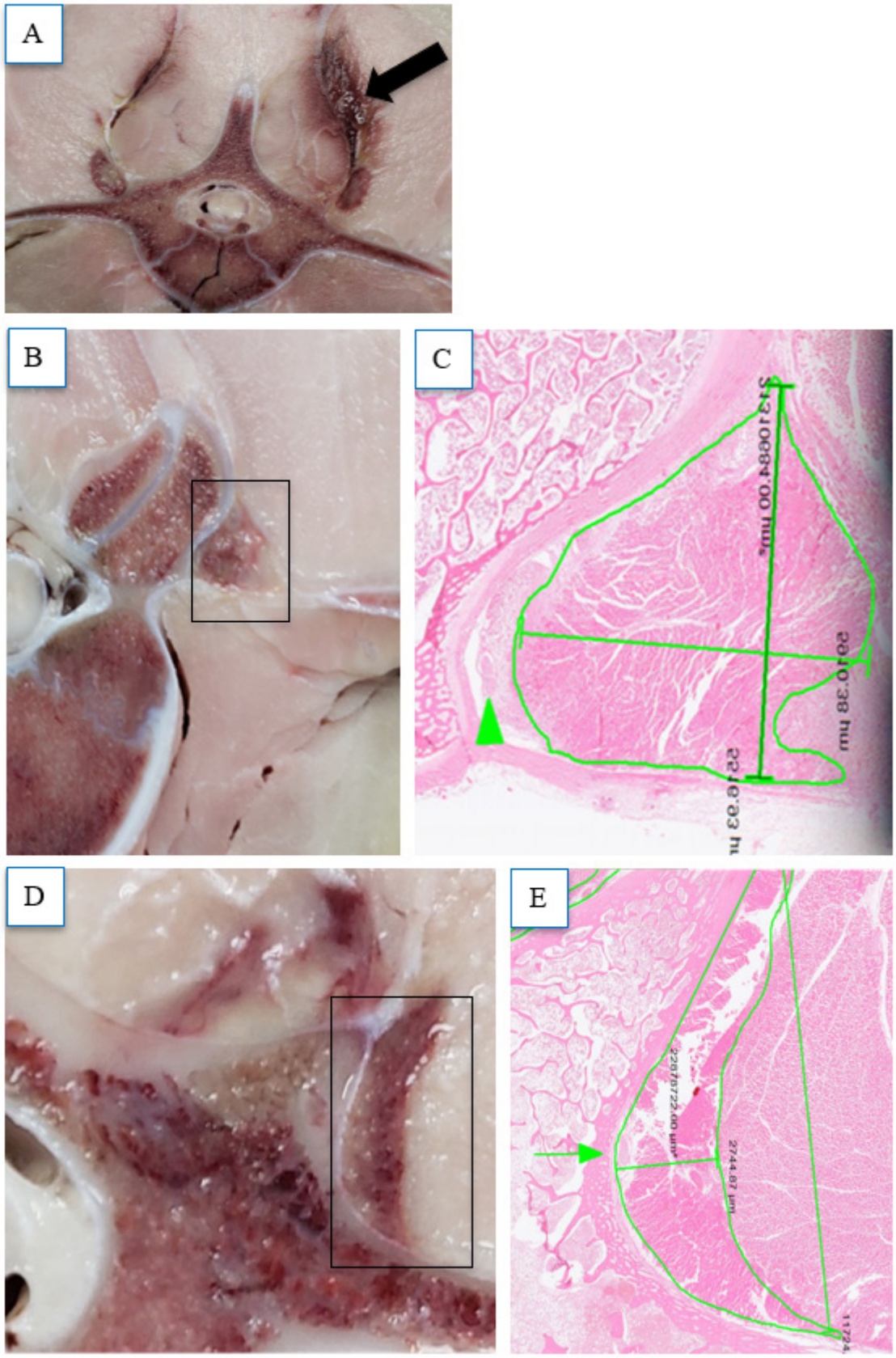

Figure 3 (A) Hemorrhage, possibly due to mechanical trauma in the paraspinal muscles (black arrow) following radiofrequency ablation (RFA). (B) Macropathology showing an area of RFA ablation near the bone (black rectangle) and (C) its corresponding micro pathology showing a viable medial branch nerve (green arrowhead) outside RFA-ablated tissue (outlined in green). (D) Macropathology of an area of high-intensity focused ultrasound (HIFU) ablation along the bony surface (black rectangle) and (E) its corresponding micropathology showing an ablated medial branch nerve (green arrow) within HIFU-ablated tissue (outlined in green).

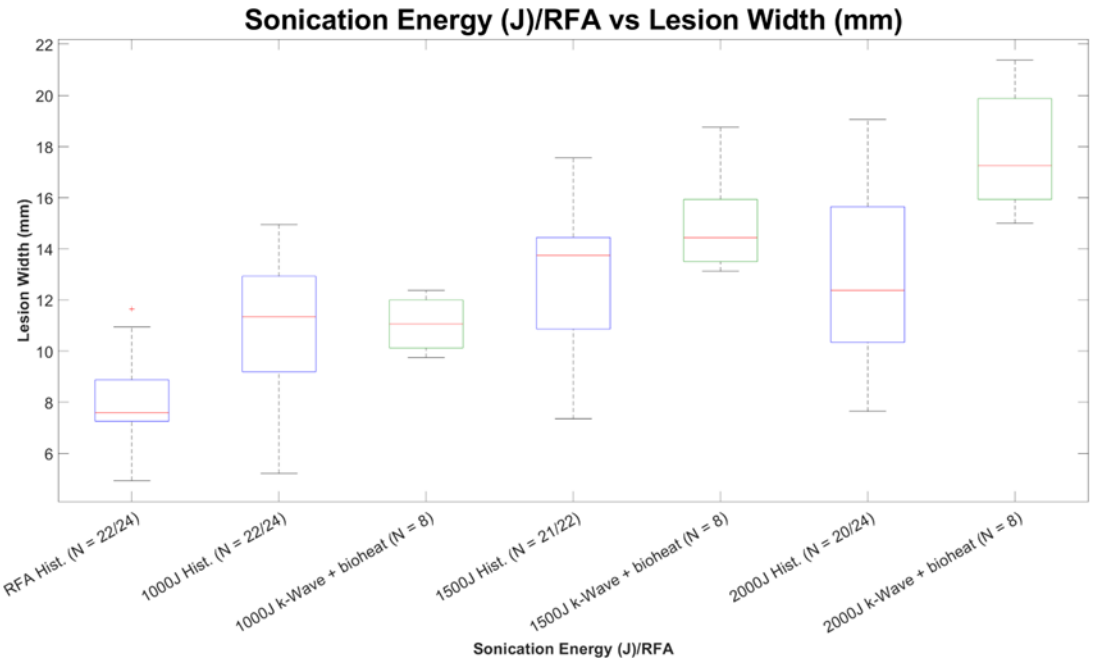

Figure 4 Comparison of lesion width on histology (blue boxes) for RFA and various HIFU energy levels compared with k-wave simulated HIFU lesions (green boxes). One simulation was performed per porcine lumbar spinal level per side, mimicking the GLP study. GLP, Good Laboratory Practice; HIFU, high-intensity focused ultrasound; RFA, radiofrequency ablation.

and reduces as it extends centrifugally. When the RFA cannula is positioned too close to a bony surface, the energy absorption by bone reduce the lesion volume, possibly leaving the nerve intact.[29] On the contrary, the HIFU lesion grows from the bone surface mostly outward, slightly inward and sideways, thereby ablating the medial branch nerves in its path with improved certainty.

The estimation of thermal damage to the targeted medial branch nerves and surrounding tissue considered the effects of heat fixation.[22–24] Heat-fixed cells are necrotic, as demonstrated by ruptured cells seen with electron microscopy, but the cells appear viable under light microscopy with H&E staining. This heat fixation phenomenon is seen in the center of an area of thermal coagulation, as occurs with HIFU. Thus, clusters of tissue, including in the evaluation of nerve viability in this study, nerves that appeared normal on H&E stain but located within the area of necrosis (as seen on histology and gross pathology), along the surface of the bone, were classified as necrotic heat-fixed. A polarized light microscopy confirmed the necrotic changes. As already mentioned, this phenomenon is distinctive with HIFU lesions that expand from the bone into the soft tissue, resulting in the nerve being in the center of the lesion most of the time. However, RFA lesions are centrifugally expanding from the tip of the probe. Protein denaturation quickly occurs next to the active tip, but the peripheral portion may never reach the desired temperatures due to the cooling effect of blood flow and fat, and rising impedance in the center. These findings can be seen in figure 3D,E, which shows a necrotic nerve within a crescent-like HIFU-ablated region and an intact nerve at the periphery of an RFA lesion (despite the RFA lesion appearing satisfactory on observation) (figure 3B,C).

When comparing HIFU histology data to simulation results, the trend of increasing lesion size with higher energies was predicted, but lesion size was overestimated in the simulation. This overestimation is due to approximations made when using a quasi-heterogeneous model and is also related to variations in lesion size along different histology cuts. Any one slide does not necessarily represent the maximum lesion width or height, while simulation will always present the maximum value; the simulation analysis is always conducted along the central axis of the acoustic beam. Therefore, simulation gives the maximal extent of the lesion, while histology may underestimate true lesion size. However, an adequate agreement was still seen between histology and simulation for lesion width.

The limitations of the study are related to the animal model. Kaye *et al*[27] reported that the average pedicle thickness in pigs was 8.5–12 mm, which is thinner than the human pedicle. The human pedicle averages 13–16 mm in females and 17–21 mm in males.[30] However, even with similar and even higher energies used in clinical studies, there were no adverse events with the thinner bones in the pigs, and the lesions created were larger than with RFA in the same animal model.

In contrast to a typical older patient with low back pain, swine multifidus muscle is strong and lacks any significant fatty infiltration, which acts as an additional electric insulator to further impede RFA size and shape. RFA lesion size may thus be overestimated in the swine model.

CONCLUSION

This animal study demonstrates a dose-dependent increase in lesion size for medial branch nerve ablation with HIFU with no adverse events. The results suggest that HIFU may be safer and more effective than conventional RFA.

The Neurolyzer XR may provide a readily accessible, safe, effective, and cost-competitive method of providing noninvasive ablation of the target nerves under fluoroscopic guidance without the need for a sterile environment and related supplies.

Acknowledgements The authors thank FUSMobile for funding the study and Jill W. Roberts, M.S., for editing assistance, and Sharon Thomsen for her help with determining the extent of heat fixation.

Contributors MG, SL, RA, and AH designed the study. MG, SM, RA and AH performed the study. RA, NR, and AH worked with the external laboratories and pathologist to acquire the data. EM, RA, SL, and AH analyzed the pathological radiological and clinical results. J-FA, TT, and EM performed the simulations and analyzed the simulation results. All team participated in writing the manuscript. MG is the guarantor.

Funding Financial support was provided by FUSMobile to cover the research costs of this study site. Data management and descriptive statistics were performed by FUSMobile.

Competing interests AH and RA are the founders of FUSMobile and hold ordinary options in the company. J-FA is a member of FUSMobile's scientific advisory board and holds ordinary options in the company. SL and EM hold shares and ordinary options in the company. SM holds ordinary options in the company. MG holds ordinary options in the company and is a consultant to the company. TT has no interests to declare.

Patient consent for publication Not applicable.

Ethics approval This study was conducted in Israel at Shamir Medical Center's Good Laboratory Practice (GLP) animal research facility and was approved by the facility's ethical review board.

Provenance and peer review Not commissioned; externally peer reviewed.

Data availability statement All data relevant to the study are included in the article or uploaded as online supplemental information.

ORCID iD

Michael Gofeld http://orcid.org/0000-0001-7372-4171

REFERENCES

1 Deyo RA, Phillips WR. Low back pain. A primary care challenge. *Spine (Phila Pa 1976)* 1996;21:2826–32.
2 Cohen SP, Bhaskar A, Bhatia A, *et al*. Consensus practice guidelines on interventions for lumbar facet joint pain from a Multispecialty, international working group. *Reg Anesth Pain Med* 2020;45:424–67.
3 Cohen SP, Raja SN. Pathogenesis, diagnosis, and treatment of lumbar Zygapophysial (facet) joint pain. *Anesthesiology* 2007;106:591–614.
4 Fitzgibbon DR, Posner KL, Domino KB, *et al*. Chronic pain management: American society of Anesthesiologists closed claims project. *Anesthesiology* 2004;100:98–105.
5 Barbieri M, Bellini M. Radiofrequency Neurotomy for the treatment of chronic pain: interference with Implantable medical devices. *Anaesthesiol Intensive Ther* 2014;46:162–5.
6 Goodman BS, House LM, Vallabhaneni S, *et al*. Anticoagulant and antiplatelet management for spinal procedures: A prospective, descriptive study and interpretation of guidelines. *Pain Med* 2017;18:1218–24.
7 Miele Frank. Ultrasound physics and instrumentation. In: *Pegasus Lectures*. 5th Edition. 2013. Available: https://pegasuslectures.com/product_info.php/products_id/52543
8 Dick EA, Gedroyc WMW. Exablate magnetic resonance-guided focused ultrasound system in multiple body applications. *Expert Rev Med Devices* 2010;7:589–97.
9 Foley JL, Eames M, Snell J, *et al*. Image-guided focused ultrasound: state of the technology and the challenges that lie ahead. *Imaging in Medicine* 2013;5:357–70.
10 Tyshlek D, Aubry J-F, Ter Haar G, *et al*. Focused ultrasound development and clinical adoption: 2013 update on the growth of the field. *J Ther Ultrasound* 2014;2:2.
11 Bradley WG. MR-guided focused ultrasound: a potentially disruptive technology. *J Am Coll Radiol* 2009;6:510–3.
12 Aubry JF. High-intensity therapeutic ultrasound: Metrological requirements versus clinical usage. *Metrologia* 2012;49:S259–66.
13 Weeks EM, Platt MW, Gedroyc W. MRI-guided focused ultrasound (Mrgfus) to treat facet joint osteoarthritis low back pain--case series of an innovative new technique. *Eur Radiol* 2012;22:2822–35.
14 Tiegs-Heiden CA, Hesley GK, Long Z, *et al*. MRI-guided focused ultrasound ablation of painful lumbar facet joints: a retrospective assessment of safety and tolerability in human subjects. *Pain Med* 2023;24:1219–23.
15 Perez J, Gofeld M, Leblang S, *et al*. Fluoroscopy-guided high-intensity focused ultrasound Neurotomy of the lumbar Zygapophyseal joints: A clinical pilot study. *Pain Med* 2022;23:67–75.
16 Chen J, LeBlang S, Hananel A, *et al*. An incoherent HIFU transducer for treatment of the medial branch nerve: numerical study and in vivo validation. *Int J Hyperthermia* 2020;37:1219–28.
17 Aginsky R, LeBlang S, Hananel A, *et al*. Tolerability and feasibility of X-ray guided non-invasive ablation of the medial branch nerve with focused ultrasound: preliminary proof of concept in a pre-clinical model. *Ultrasound in Medicine & Biology* 2021;47:640–50.
18 Treeby BE, Cox BT. K-wave: MATLAB Toolbox for the simulation and reconstruction of Photoacoustic wave fields. *J Biomed Opt* 2010;15:021314.
19 Sapareto SA, Dewey WC. Thermal dose determination in cancer therapy. *Int J Radiat Oncol Biol Phys* 1984;10:787–800.
20 Schlesinger D, Lee M, Ter Haar G, *et al*. Equivalence of cell survival data for radiation dose and thermal dose in Ablative treatments: analysis applied to essential tremor thalamotomy by focused ultrasound and gamma knife. *Int J Hyperthermia* 2017;33:401–10.
21 Yarmolenko PS, Moon EJ, Landon C, *et al*. Thresholds for thermal damage to normal tissues: an update. *Int J Hyperthermia* 2011;27:320–43.
22 Wu F, Wang Z-B, Cao Y-D, *et al*. Heat fixation of cancer cells ablated with high-intensity-focused ultrasound in patients with breast cancer. *Am J Surg* 2006;192:179–84.
23 Anttinen M, Yli-Pietilä E, Suomi V, *et al*. Histopathological evaluation of prostate specimens after thermal ablation may be confounded by the presence of thermally-fixed cells. *Int J Hyperthermia* 2019;36:915–25.
24 Courivaud F, Kazaryan AM, Lund A, *et al*. Thermal fixation of swine liver tissue after magnetic resonance-guided high-intensity focused ultrasound Ablation1. *Ultrasound in Medicine & Biology* 2014;40:1564–77.
25 Harnof S, Zibly Z, Shay L, *et al*. Magnetic resonance-guided focused ultrasound treatment of facet joint pain: summary of Preclinical phase. *J Ther Ultrasound* 2014;2:9.
26 Krug R, Do L, Rieke V, *et al*. Evaluation of MRI protocols for the assessment of lumbar facet joints after MR-guided focused ultrasound treatment. *J Ther Ultrasound* 2016;4:14.
27 Kaye EA, Monette S, Srimathveeravalli G, *et al*. MRI-guided focused ultrasound ablation of lumbar medial branch nerve: feasibility and safety study in a swine model. *Int J Hyperthermia* 2016;32:786–94.
28 Haines D. *Catheter Ablation of Cardiac Arrhythmias*Fourth Edition. Elsevier, 2020.
29 Desai MJ, Safriel Y. Mri for in vivo analysis of ablation zones formed by cooled radiofrequency Neurotomy to treat chronic joint pain across multiple axial spine sites. *J Pain Res* 2022;15:423–30.
30 Zwiebel H, Aginsky R, Hananel A, *et al*. In vivo measurements of medial branch nerve depth and adjacent osseous structures for ablation of facet-related back pain: predictors for patient candidacy. *North American Spine Society Journal (NASSJ)* 2020;3:100018.